Indoor Localization of UAVs Using Only Few Measurements by Efficient Preimage Approximation - Supplementary Materials

Michael M. Bilevich[†] Tomer Buber[†] Dan Halperin[†]

1 Proofs for the correctness of the voxel intersection predicate

In this section, we complete some details regarding the correctness of the voxel intersection predicate, defined as follows. Recall that during our subdivision search for the preimage intersection, we need to query whether some voxel V indeed intersects all preimages. We then show that this query is equivalent to querying whether a given solid $F_d \circ g(V)$ intersects the environment $\mathcal{W}$. This query is referred to as the *voxel intersection query.*

1.1 The shape of $F_d \circ g(V)$

Recall the definition of the function $F_d : \mathbb{R}^3 \times \mathbb{S}^1 \to \mathbb{R}^3$,

$$F_d(x,y,z,\theta) = (x,y,z-d). \tag{1}$$

We then prove the following useful lemma:

Lemma 1.1. *For any voxel V, $V \cap M_{d_i,\bar{g}_i} \neq \emptyset$ if and only if $F_d \circ g(V) \cap \mathcal{W} \neq \emptyset$.*

Proof. A point $q \in V$ is also $q \in M_{d_i,\bar{g}_i}$ if and only if a ray emanating from the sensor at pose $g(q)$ measures distance d (by definition of $M_{d_i,\bar{g}_i}$), hence the intersection of that ray with the environment is at distance d, if and only if that intersection point is $F_d \circ g(q)$. □

We then recall that for any subset $A \subset \mathbb{R}^3$, $F_d(A) = A \oplus \{-d \cdot \vec{e}_z\}$, with $\vec{e}_z = (0,0,1,0)$ and $\oplus$ is the Minkowski sum, and for a voxel V,

$$F_d \circ g(V) = \pi_{xyz}(g(V)) \oplus \{-d \cdot \vec{e}_z\}, \tag{2}$$

hence it suffices to describe the geometry of $\pi_{xyz}(g(V))$.

Theorem 1.2. *For a transformation $g \in \mathbb{R}^3 \times \mathbb{S}^1$, define $\gamma_g : \mathbb{S}^1 \to \mathbb{R}^2$ as*

$$\gamma_g(\theta) = ||\pi_{xy}(g)|| e^{i(\theta + \arctan \frac{g_y}{g_x})} \in \mathbb{C} \simeq \mathbb{R}^2. \tag{3}$$

Then:

$$\pi_{xyz}(g(V)) = \pi_{xyz}(V) \oplus (\gamma_g(\pi_\theta(V)) \times \{g_z\}). \tag{4}$$

Proof. Follows immediately from the definition of g as a sum of the different components, and the fact that

$$\gamma_g(\theta) = (g_x \cos\theta - g_y \sin\theta, g_x \sin\theta + g_y \cos\theta). \tag{5}$$

We omit the straightforward trigonometric analysis. □

We are then tasked with determining this two-dimensional shape, which is the Minkowski sum of a circular arc with a square $\pi_{xy}(V)$.

[†]Blavatnik School of Computer Science, Tel-Aviv University, Israel. This work has been supported in part by the Israel Science Foundation (grant no 2261/23), by NSF/US-Israel-BSF (grant no. 2019754), by the Blavatnik Computer Science Research Fund, and by the Shlomo Shmelzer Institute for Smart Transportation at Tel Aviv University.

Definition 1.1. *For any vector $v \in \mathbb{R}^2$, a curve $\gamma : I \to \mathbb{R}^2$ is said to be v-*monotone *if $\pi_v \circ \gamma : I \to \mathbb{R}$ is monotone, with $\pi_v : \mathbb{R}^2 \to \mathbb{R}$ a projection onto the vector v.*

Lemma 1.3. *Assume that $\gamma_g(\pi_\theta(V))$ is contained exactly in one quadrant of $\mathbb{S}^1$. Then $\pi_{xy}(V) \oplus \gamma_g(\pi_\theta(V))$ is simply connected.*

Proof. We note that if $\gamma_g(\pi_\theta(V))$ is contained exactly in a single quadrant of $\mathbb{S}^1$, then it is both x and y-monotone. Hence the mapping $\Gamma_v : I \times I \to \mathbb{R}^2$, defined by $\Gamma_v(s,t) = p + t \cdot v + \gamma_g(\pi_\theta(s))$ is a homeomorphism on its image for both $v = \vec{e}_x$ and $\vec{e}_y$. For any loop in $\pi_{xy}(V) \oplus \gamma_g(\pi_\theta(V))$, be sweeping along the x-axis, we can contract each point upwards (since $\Gamma_y(I \times I)$ is simply connected), hence the loop is homotopic to a loop contained in $\Gamma_x(I \times I)$, which is also simply connected. Hence every loop in $\pi_{xy}(V) \oplus \gamma_g(\pi_\theta(V))$ is contractible. $\square$

Finally, we have a complete description of the solid $F_d \circ g(V)$, which we can intersect with our environment $\mathcal{W}$. However, we note that is it simpler (computationally) to efficiently query if an axis aligned box intersects with the environment. We note that besides the rounded corners of $F_d \circ g(V)$, this solid resembles an axis aligned box. Hence we can instead take its bounding box (or a union of at most four bounding boxes, if $\gamma_g(\pi_\theta(V))$ is not contained in a single quadrant) as an approximation of our solid, for faster queries. If we would like a precise query, we can instead take $F_d \circ g(V)$ itself. In the Supplementary Material, we compute the difference between the volume of the solid $F_d \circ g(V)$ and its bounding box, and argue that it is not large for sufficiently small δ.

1.2 The difference in volume between the solid $F_d \circ g(V)$ and its bounding box

In our implementation, instead of explicitly representing the solid $F_d \circ g(V)$, we compute its bounding box. In this section we compute the difference in volume between the two. We will compute the difference between the two-dimensional shape $\pi_{xy}(V) \oplus \gamma_g(\pi_\theta(V))$ and its bounding rectangle. We denote this difference by Δ_{xy}. The difference between volume of the solid $F_d \circ g(V)$ and its bounding box, denoted by Δ, will then be the difference between the two dimensional shapes Δ_{xy}, times the height of the box.

Lemma 1.4. *Denote the angle interval by $\pi_\theta(V) = [\theta_0, \theta_1)$. Then $\Delta_{xy} = O(\theta_1 - \theta_0)$.*

Proof. We first note that the difference Δ_{xy} is the sum of the area bellow the circular arc, and above the circular arc. See Figure 1 for an illustration. Hence it is the area of a bounding box of that circular arc:

$$\Delta_{xy} = ||\pi_{xy}(g)||^2 \cdot (\gamma_{1x} - \gamma_{0x}) \cdot (\gamma_{1y} - \gamma_{0y}) \tag{6}$$

$$= ||\pi_{xy}(g)||^2 \cdot \left(\cos(\theta_1 + \arctan\frac{g_y}{g_x}) - \cos(\theta_0 + \arctan\frac{g_y}{g_x}) \right) \cdot \tag{7}$$

$$\left(\sin(\theta_1 + \arctan\frac{g_y}{g_x}) - \sin(\theta_0 + \arctan\frac{g_y}{g_x}) \right). \tag{8}$$

Using trigonometric identities, we can simplify:

$$\Delta_{xy} = -4||\pi_{xy}(g)||^2 \cdot \cos\frac{\theta_1 - \theta_0}{2} \cdot \sin\frac{\theta_1 - \theta_0}{2} \cdot \tag{9}$$

$$\cos\frac{\theta_0 + \theta_1 + 2\arctan\frac{g_y}{g_x}}{2} \cdot \sin\frac{\theta_0 + \theta_1 + 2\arctan\frac{g_y}{g_x}}{2}. \tag{10}$$

Finally, we can take the inequality:

$$\Delta_{xy} \leq 4||\pi_{xy}(g)||^2 \left| \sin\frac{\theta_1 - \theta_0}{2} \right|, \tag{11}$$

$$\lim_{\delta \to 0} \frac{\Delta_{xy}}{(\theta_1 - \theta_0)/2} \leq \lim_{\delta \to 0} 4||\pi_{xy}(g)||^2 \cdot \frac{|\sin((\theta_1 - \theta_0)/2)|}{(\theta_1 - \theta_0)/2} = 4||\pi_{xy}(g)||^2 < \infty. \tag{12}$$

$\square$

Corollary 1.1. *Denote the z-interval by $\pi_z(V) = [z_0, z_1)$. Then $\Delta = O((z_1 - z_0) \cdot (\theta_1 - \theta_0))$.*

We finally note that since $(\theta_1 - \theta_0), (z_1 - z_0) \leq \delta$, we also get that $\Delta = O(\delta^2)$.

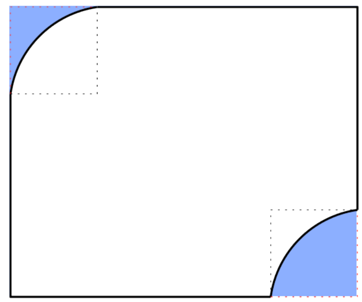

Figure 1: Illustration of the difference in area between the top face of $F_d \circ g(V)$ and its bounding rectangle. The difference is colored in blue. Note that sum of both blue areas comprises the area of a single bounding rectangle of the circular arc.

2 Full analysis of the time complexity

First, we formally define the notions of Hausdorff measure and dimensions. Then, we prove the result of the time complexity of our method.

Recall the notion of the *Lebesgue measure* of a set, which is defined, intuitively, as the infimum over the volume of a union of boxes which cover that set. One can show that sub-manifolds of co-dimension ≥ 1 are sets of Lebesgue measure zero. Nonetheless, some sets, such as the aforementioned manifolds, have a non-zero "measure", sometimes referred to as area or length. The notion of *Hausdorff measure* extends this idea of measure to general sets, given some parameter d, called the *dimension*. The d-dimensional Hausdorff measure of a set, is defined roughly, as the infimum over the "d-dimensional-volume" of covers of that set. The n-dimensional volume of a cube in $\mathbb{R}^n$ is (up to a constant), the diameter of the cube, to the power of n.

For example, the 1-dimensional Hausdorff measure of a curve embedded in $\mathbb{R}^n$ is its length, and the 2-dimensional Hausdorff measure of a two-dimensional manifold embedded in $\mathbb{R}^3$ is its surface area. The n-dimensional Hausdorff measure coincides, up to a constant, with the Lebesgue measure on $\mathbb{R}^n$. Finally, note that this dimension d does not necessarily have to be integer. In fact, some sets can be shown to have a fractional Hausdorff dimension, with non-zero measure. In this work however, we consider integeral valued dimensions.

Definition 2.1. *For $A \subset \mathbb{R}^n$, $0 \leq d < \infty$, $0 < \varepsilon \leq \infty$, and $\{B_j\}_j$ any countable collection of subsets of $\mathbb{R}^n$. Denote by $\operatorname{diam}(B)$ is the diameter of some set B. Then define the d-dimensional-volume of the collection $\{B_j\}_j$ as,*

$$\mu^d(\{B_j\}_j) := \sum_{j=1}^{\infty} (\operatorname{diam} B_j)^d, \tag{13}$$

and the ε-d-Hausdorff measure as the infimum of d-dimensional volumes covering the set A, where each subset B_j is at most ε-wide:

$$\mathcal{H}^d_\varepsilon(A) := \inf \left\{ \mu^d(\{B_j\}_j) \middle| A \subseteq \bigcup_{j=1}^{\infty} B_j, \operatorname{diam} B_j \leq \varepsilon \right\}. \tag{14}$$

Taking $\varepsilon \to 0$, we get the Hausdorff d-dimensional measure*:*

$$\mathcal{H}^d(A) := \lim_{\varepsilon \to 0} \mathcal{H}^d_\varepsilon(A) = \sup_{\varepsilon > 0} \mathcal{H}^s_\varepsilon(A). \tag{15}$$

The Hausdorff dimension *of a set $A \subset \mathbb{R}^n$ is:*

$$\mathcal{H}_{\dim}(A) := \inf\{0 \leq s < \infty | \mathcal{H}^s(A) = 0\}. \tag{16}$$

We also recall the following result:

Theorem 2.1. *For a set $A \subset \mathbb{R}^n$, if $\mathcal{H}_{\dim}(A) = d$, then $\forall 0 \leq s < d$, $\mathcal{H}^s(A) = 0$, $\forall s > d, \mathcal{H}^s(A) = \infty$ and $0 < \mathcal{H}^d(A) < \infty$.*

In this work, at each iteration ℓ we have a collection of active voxels, denoted by $C_\ell = \{V_\ell^{(j)}\}_j$ with $\mathrm{diam} V_\ell^{(j)} = \frac{\delta_0}{2^\ell}$ and δ_0 is the diameter of the bounding box V_0. We also note that $\bigcap_{i=1}^k M_{d_i,\bar{g}_i} \subseteq \bigcup_j V_\ell^{(j)}$, and $\bigcap_{i=1}^k M_{d_i,\bar{g}_i} = \bigcap_{\ell=1}^\infty \bigcup_j V_\ell^{(j)}$.

We now present the analysis of the time complexity.

Theorem 2.2. *Assume that evaluating the voxel intersection predicate takes at most $\mathcal{Q}_\mathcal{W}$ time, where $\mathcal{Q}_\mathcal{W}$ depends only on the combinatorial complexity of the environment. Denote $\cap M_i := \bigcap_{i=1}^k M_{d_i,\bar{g}_i}$ with $\mathcal{H}_{\dim}(\cap M_i) = d$. Then our method is*

$$\Theta\left(k \cdot \mathcal{Q}_\mathcal{W} \cdot \log\delta \cdot \frac{\mathcal{H}^d(\cap M_i)}{(\delta_0 \cdot \delta)^d}\right). \tag{17}$$

Proof. Notice that $\mu^d(C_\ell) = |C_\ell| \cdot \left(\frac{\delta_0}{2^\ell}\right)^d$. Since [1] $\lim_{\ell\to\infty} C_\ell = \cap M_i$, we have:

$$\mathcal{H}^d(\cap M_i) = \lim_{\ell\to\infty} \mu^d(C_\ell) = \lim_{\ell\to\infty} |C_\ell| \cdot \left(\frac{\delta_0}{2^\ell}\right)^d \tag{18}$$

Hence the number of voxels $|C_\ell|$ at each iteration ℓ is $\Theta\left((\delta_0 \cdot 2^{-\ell})^{-d}\right)$. For each voxel, we perform a query that takes $\theta(k \cdot \mathcal{Q}_\mathcal{W})$ time. Finally, we have $\ell \leq \log\delta$ such iterations, and we get the desired time complexity. □

References

[1] L. Evans, *Measure theory and fine properties of functions.* Routledge, 2018.